Biosensors and Bioelectronics 65 (2015) 23–30

Contents lists available at ScienceDirect

Biosensors and Bioelectronics

journal homepage: www.elsevier.com/locate/bios

An ultra-sensitive acetylcholinesterase biosensor based on reduced graphene oxide-Au nanoparticles-β-cyclodextrin/Prussian blue-chitosan nanocomposites for organophosphorus pesticides detection

Haiyan Zhao [a], Xueping Ji [a,*], Beibei Wang [a], Na Wang [a], Xianrui Li [a], Ruixing Ni [a], Jujie Ren [b,*]

[a] Department of Medical Chemistry, Hebei Medical University, Shijiazhuang 050017, China
[b] Department of Chemistry, School of Sciences, Hebei University of Science and Technology, Shijiazhuang 050018, China

ARTICLE INFO

Article history:
Received 31 July 2014
Received in revised form
24 September 2014
Accepted 2 October 2014
Available online 6 October 2014

Keywords:
Acetylcholinesterase
Electrochemical reduced graphene oxide
Au nanoparticles
Prussian blue
Biosensor
Organophosphorus pesticides

ABSTRACT

This work reports a novel, ultrasensitive, and selective sensing platform based on a direct electrodeposition of electrochemical reduced graphene oxide (ERGO)-Au nanoparticles (AuNPs)-β-cyclodextrin (β-CD) and Prussian blue-chitosan (PB-CS) on glass carbon electrode (GCE) for efficiently fixed acetylcholinesterase (AChE) to fabricate organophosphorus pesticides (OPs) biosensor. The PB-CS not only effectively catalyzed the oxidation of thiocholine (TCh), but also shifted its oxidation potential from 0.68 to 0.2 V, and accordingly the sensitivity of the biosensor was obviously improved. The synergistic effect between ERGO and AuNPs significantly promoted the electron transfer between PB and GCE, and remarkably enhanced the electrochemical oxidation of TCh. Besides, β-CD could interact with substrate by reversible bonding, which is contribute to increase the enrichment of the substrate and improve the selectivity and sensitivity of the biosensor. The integration of ERGO-AuNPs-β-CD with PB-CS provided an advantageous and high-performance platform for sensing applications. Based on the inhibition of OPs on AChE activity, the sensor showed wide linear ranges of $7.98-2.00\times10^3$ pg mL^{-1} and $4.3-1.00\times10^3$ pg mL^{-1} with low detection limits of 4.14 pg mL^{-1} and 1.15 pg mL^{-1} for malathion and carbaryl, respectively. The proposed biosensor exhibited short response time, good stability and high sensitivity, which can be used for direct analysis of practical samples.

1. Introduction

Organophosphorus pesticides (OPs) are extensively used in the field of agriculture owing to their high insecticidal activity. However pesticide residues threat human health due to their high toxicity to acetylcholinesterase (AChE), which is essential for the function of central nervous system in humans (Abad et al., 1998; Du et al., 2008). Therefore, for human health safety and environmental protection purposes, it is of great significance to develop a fast, reliable and economical analytical method for ultra-trace pesticide detection. Comparison with the conventional analytical methods, such as liquid chromatography (Ye et al., 2009), gas chromatography (Guan et al., 2010), and enzyme-linked immunoabsorbant assays (Rekha et al., 2000), electrochemical biosensors with advantages of fast response, high sensitivity, low cost, miniaturization, and on-site analysis, have been a promising alternative to rapidly detect pesticides. Among them, AChE based electrochemical biosensors are particularly attractive due to their fast response and high sensitivity (Zhou et al., 2013; Li et al., 2013). The AChE immobilized on an electrode surface can catalyze the hydrolysis of acetylthiocholine chloride (ATCl) to produce an electro-active product of thiocholine (TCh), which shows an irreversible oxidation peak at about 0.68 V (Liu and Lin, 2006; Ivanov et al., 2003) as a marker for pesticide detection. However, the oxidation peak of TCh, with a high oxidation potential, is very weak, which result in poor sensitivity. Therefore, improving the performance of the biosensors and decreasing oxidation potential of TCh have been the research focus of AChE based electrochemical biosensors.

Recent years, various nanomaterials have been widely employed to improve the performance of electrode interface. Graphene, a kind of nanomaterial with a monolayer of sp^2 hybridized carbon atoms (Novoselov et al., 2004; Allen et al., 2010), has especially attracted increasing research interests due to its remarkable properties (Kim et al., 2009), such as extremely high thermal conductivity, high mobility of charge carriers, high surface

* Corresponding authors.
E-mail addresses: xuepingji@126.com, xpji03@yahoo.com.cn (X. Ji), renjujie@yahoo.com (J. Ren).

http://dx.doi.org/10.1016/j.bios.2014.10.007
0956-5663/

area-to-volume ratio and good biocompatibility. The unique properties of graphene give it potential applicability in electrochemical biosensors (Brownson and Banks, 2010). Graphene is generally synthesized by chemical reduction of exfoliated graphite oxide (GO) in solution using different reducing agents. In order to prevent aggregation of graphene in aqueous medium, other molecules or polymers as the stabilizers are usually attached onto the graphene to improve solubility (Liu et al., 2010a, 2010b; Guo et al., 2010). However, the introduction of foreign stabilizers is generally undesirable and time-consuming for most applications. By comparison with chemical synthesis, graphene prepared using electrochemical deposition is simple, time-saving, nontoxic and green nature, with controllable thickness and good reproducibility. More recently, it is interesting to develop graphene-based nanocomposites as enhanced sensing platform for sensor design (Sun et al., 2011; Bai et al., 2013). Typically, some semiconductor and conductor nanomaterials, such as CdS (Wu et al., 2013), multiwalled carbon nanotubes (Sun et al., 2013), Au (Song et al., 2013) and Prussian blue (PB) nanoparticles (Yang et al., 2012), have been incorporated with graphene for the construction of electrochemical biosensors. These kinds of nanocomposites films can generate synergy on electrocatalytic activity and improve the sensitivity of the sensors (Liu et al., 2010a, 2010b; Zhou et al., 2010). Also Au nanaoparticles (AuNPs) can be prepared by eletrochemical methods, so it is possible to synthesis of graphene–AuNPs by one step co-eletrodeposition method. The introduction of AuNPs can not only improve the conductivity of graphene, but also prevent its agglomeration.

PB, as a mediator, could oxidize TCh that generated from the hydrolysis of ATCl catalyzed by AChE at low potential (Arduini et al., 2006; Ricci et al., 2004). The PB nanocomposites prepared using electrochemical deposition is fresh, with controllable thickness and good reproducibility (Tan et al., 2010). Nevertheless, a pure PB electrodeposited film is still easy to decompose, and displays poor cycling stability at neutral solution on the electrode surface (Chiu et al., 2009). The co-electrodeposition of PB combined with chitosan (CS) to the electrode surface can solve this problem. CS, a polyelectrolyte with amino groups, can not only make PB stable in neutral solution and maintain its high activity, but also avoid PB leakage (Song et al., 2011; Wang et al., 2014).

Additionally, compatible β-cyclodextrin (β-CD), containing hydroxyl groups, can interact with graphene via strong hydrogen-bonding interaction and prevent the agglomeration of graphene (Morozov et al., 2008). Besides, β-CD can interact with acetylcholine by reversible bonding, which is contribute to increase the enrichment of acetylcholine, and improve the selectivity and sensitivity of the OPs biosensor (Lee et al., 2008). ATCl and acetylcholine have a similar configuration, so there is a reason to expect the β-CD can also be combined with ATCl by reversible bonding.

So far, even though graphene, AuNPs, and PB-CS composite have been extensively applied for the construction of sensing interface, there is not a report that integrates the electrochemical reduced graphene oxide (ERGO)-AuNPs-β-CD and PB-CS for the application in AChE biosensors yet.

This work proposed one-step direct electrodeposition approach to synthesis of ERGO-AuNPs-β-CD on glassy carbon electrode (GCE), and followed by the co-electrodeposition of PB-CS composites. This direct electrodeposition approach for the construction of ERGO-based hybrid film was simple, quick and environmentally friendly. ERGO-based composites could present a large surface area for AChE adsorption, and the synergy of AuNPs and ERGO could increase electron transfer obviously and enhance the signal of electro-oxidation of TCh. The introduction of PB-CS could reduce the overpotential and improve the selectivity of the biosensor. Encouragingly, the integration of ERGO-AuNPs-β-CD with PB-CS may open up new opportunities for fast, simple and sensitive analysis of OPs.

2. Experimental

2.1. Reagents

Graphite powder was provided by Sinopharm Chemical Reagent Co. Ltd. (China). Acetylcholinesterase (518 unit mg^{-1}), acetylthiocholine chloride, malathion, carbaryl, chloroauric acid trihydrate ($HAuCl_4 \cdot 3\,H_2O$) and pralidoxime iodide, obtained from Sigma, were used without further purification. Chitosan (MW 1.5×10^5, 75%–85% deacetylation) was purchased from Yuhuan Chemical Factory (Zhejiang, China). β-Cyclodextrin was provided by Tianjin Bodi Chemical Co. Ltd. (China). All other chemicals and reagents were of analytical grade, and used as received.

GO was synthesized from graphite powder by Hummers and Offeman (1958) method, and it was characterized by UV–vis absorption spectra and X-ray diffraction (XRD) (shown in Fig. S1). The obtained aqueous dispersion of GO sheet (2 mg mL^{-1}) was stored at 4 °C for further use.

A 1.0 wt% CS solution was prepared by the same method in a previous paper (Wang et al., 2014). Phosphate buffer solutions (PBS, 0.1 M, pH 6.5) were used for all electrochemical studies.

2.2. Apparatus

Electrochemical experiments were performed using a computer-controlled CHI 750C electrochemical workstation (CH Instruments, Chenhua Co., Shanghai, China) at room temperature with a three-electrode system. The working electrode was a modified GCE. The reference electrode and the counter electrode were a Ag/AgCl (3 M KCl) and a platinum wire, respectively.

UV–vis spectrophotometer (TU-1901, Purkinje General Instrument Co. Ltd., Beijing, China) and X-ray diffraction spectrometer (D/MAX-2500, Japan) were used for the characterization of GO. Surface morphology of the modified electrodes was characterized by a scanning electron microscope (SEM, S-4800, Japan).

2.3. Preparation of modified electrode

The bare GCE (3 mm Φ) was polished with 1200 grit Carbimet disk, followed by 1.0, 0.3 and 0.05 μm alumina slurry. After being rinsed thoroughly with water between each polishing step, the electrode was sequentially sonicated with a fresh solution (HNO_3:H_2O=1:1 (v/v)) for 5 min, ethanol for 3 min and water for 3 min. After being rinsed with water and dried at room temperature, an aliquot of 15 μL GO aqueous dispersion was dropped on the surface of the electrode and dried in air. Then, one-step electrochemical deposition of ERGO-AuNPs-β-CD on the electrode was performed by chronoamperometry in a stirred 0.1 M PBS containing 1.25 mM $HAuCl_4$ and 0.15 mg mL^{-1} β-CD at a fixed potential of −1.4 V for 720 s. After that, PB-CS was electrochemically deposited on the ERGO-AuNPs-β-CD-modified electrode by cyclic voltammetry (CV) in an unstirred fresh 0.5 mM $K_3[Fe(CN)_6]$ +0.5 mM $FeCl_3$+0.01% CS solution (containing 0.1 M KCl and 0.01 M HCl) in the potential range of −0.1 − 0.45 V for 10 cycles at a scan rate of 20 mV s^{-1}. After dried in air, a 10 μL of 0.5 mg mL^{-1} AChE solution was coated on the PB-CS/ERGO-AuNPs-β-CD-modified GCE and dried in a refrigerator at 4 °C. Finally, a 10 μL of CS solution was dropped on the surface of AChE/PB-CS/ERGO-AuNPs-β-CD/GCE electrode and nearly dried. The fabricating processes of the biosensor are shown in Scheme S1. The resulting electrode was stored in 0.1 M PBS (pH 6.5) at 4 °C for future use.

2.4. Measurement procedure

The proposed electrode was employed for the determination of pesticides using DPV at 0.2 V. For inhibition tests, the original DPV signal was first recorded in 0.1 M PBS containing 10.0 mM ATCl, and then the electrode was incubated in a given concentration of pesticide for 10 min. After inhibition, the residual signal was measured at the same condition as the original DPV measurement. The inhibition rate of pesticide was calculated as follows.

$$\text{Inhibition}(\%) = \left(I_{\text{P,control}} - I_{\text{P,exp}}\right)/I_{\text{P,control}} \times 100\%$$

where $I_{\text{P,control}}$ is the peak current of ATCl without pesticide inhibition and $I_{\text{P,exp}}$ is the peak current of ATCl with pesticide inhibition. Inhibition (%) was plotted against the concentration of the pesticide to obtain linear calibration graph.

3. Results and discussion

3.1. Characterization of ERGO-AuNPs-β-CD nanocomposite film

SEM was employed to characterize the morphology of ERGO and ERGO-AuNPs-β-CD modified electrodes, and the SEM images are shown in Fig. 1(A, B). Fig. 1(A) displays the modality of ERGO electrodeposited on the GCE. A uniform layer structure of ERGO film was spread out on the surface of the electrode, showing the stacks of wrinkled multilayer graphene (Gan and Hu, 2011). Fig. 1 (B) exhibits the SEM image of the ERGO-AuNPs-β-CD modified GCE and the top left inset displays the magnified view of the nanosheets. The size and shape of each AuNPs can be observed clearly. Large amounts of AuNPs were embedded or wrapped on the wrinkled graphene sheets, which minimized the barrier of the electron transfer between layers and resulted in the excellent electrochemical property.

Electrochemical properties of different nanomaterials-modified electrodes were further characterized by CV. Fig. 1(C) shows the cyclic voltammograms (CVs) of bare GCE, and AuNPs-β-CD, ERGO-β-CD and ERGO-AuNPs-β-CD modified GCE in 0.1 M PBS containing 5 mM $K_3[Fe(CN)_6]/K_4[Fe(CN)_6]$. On the bare GCE (curve a), a pair of well-defined redox peaks, characteristic of a diffusion-limited redox process, was observed. When AuNPs-β-CD was electrodeposited on GCE, the peak currents increased apparently (curve b). This may contribute to the excellent conductivity of AuNPs, which can act as an electron conducting tunnel or electrical wire and promote the transmission of electrons between the redox probe and the underlying electrode (Ou et al., 2007; Zhao et al., 2006). On the ERGO-β-CD-modified GCE, the peak currents also increased (curve c), due to the excellent electric conductivity of ERGO, which can promote the transmission of electrons. Moreover, when ERGO and AuNPs with β-CD were co-electrodeposited on GCE (ERGO-AuNPs-β-CD/GCE), a dramatic increase of the peak currents was observed (curve d), compared with AuNPs-β-CD/GCE or ERGO-β-CD/GCE. The results indicated that the combination of ERGO and AuNPs further improved the

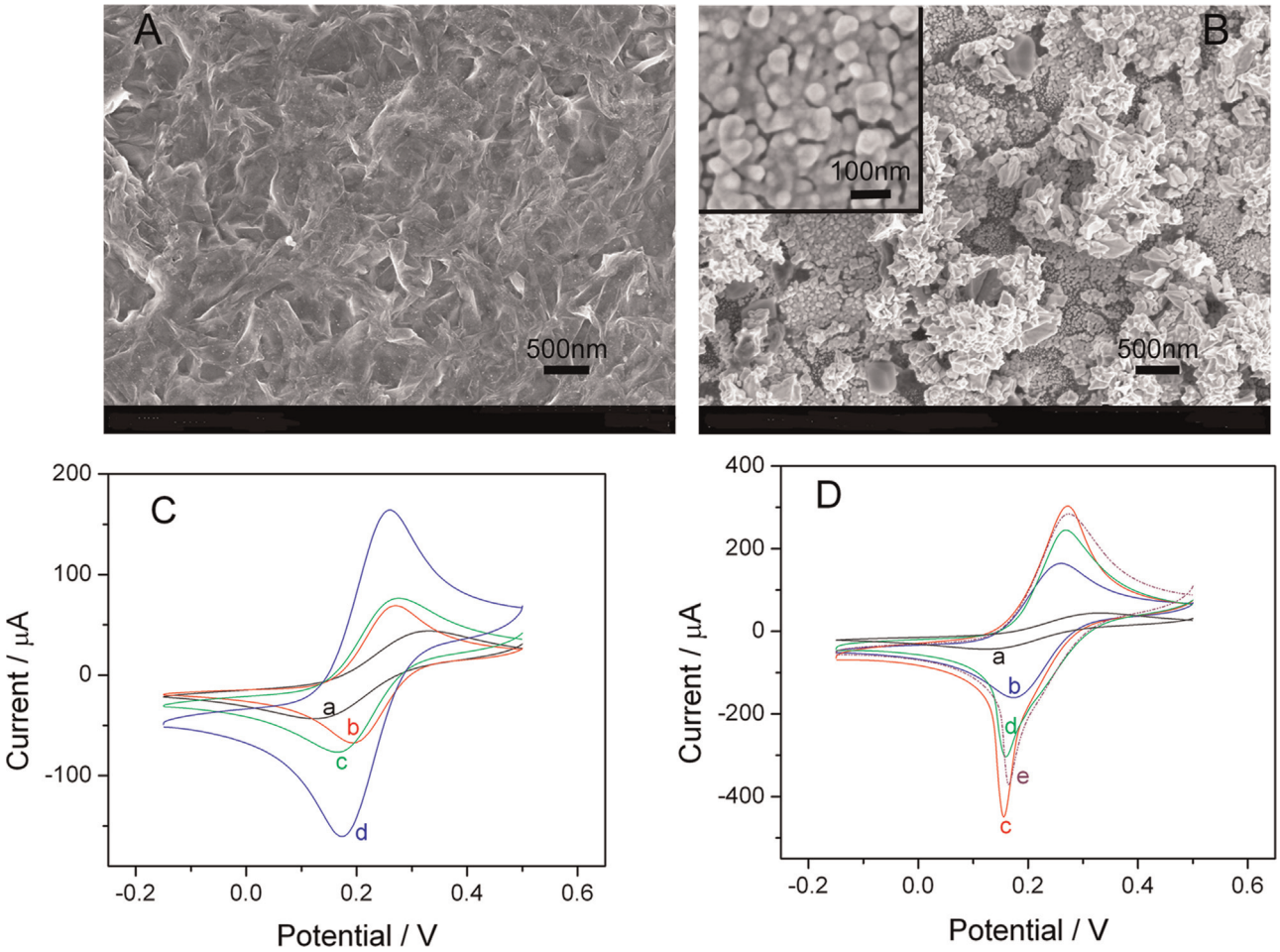

Fig. 1. SEM images of ERGO film (A) and ERGO-AuNPs-β-CD film (B). (C) CVs of bare GCE (a), AuNPs-β-CD/GCE (b), ERGO-β-CD/GCE (c) and ERGO-AuNPs-β-CD/GCE (d), and (D) CVs of bare GCE (a), ERGO-AuNPs-β-CD/GCE (b), PB-CS/ERGO-AuNPs-β-CD/GCE (c), AChE/PB-CS/ERGO-AuNPs-β-CD/GCE (d) and CS/AChE/PB-CS/ERGO-AuNPs-β-CD/GCE (e) in 0.1 M PBS (pH 6.5) containing 5 mM $K_3[Fe(CN)_6]/K_4[Fe(CN)_6]$ at a scan rate of 20 mV s^{-1}.

electronic transport due to the presence of synergistic effect between them (Hu et al., 2010).

3.2. Electrochemical characterization of enzyme electrode

The assembly process of the enzyme electrode was monitored by CV. Fig. 1(D) shows the CVs in 0.1 M PBS containing 5 mM $K_3[Fe(CN)_6]/K_4[Fe(CN)_6]$ at different modified electrodes. A pair of well-defined redox peaks was observed at the bare GCE in the potential range from −0.15 to 0.5 V (curve a). When ERGO-AuNPs-β-CD was electrodeposited on GCE, the peak currents increased apparently (curve b). This may be contributed to the synergy of ERGO and AuNPs nanocomposites, which improve the conductivity of the whole electrode surface (Hu et al., 2010). After the assembling of PB-CS on the ERGO-AuNPs-β-CD film, the peak currents further increased (curve c). This may be ascribed to the conversion between Prussian white (PW) and PB (Zeng et al., 2008). After AChE was coated on the electrode (curve d), the peak currents obtained were smaller than that of enzyme-free electrode. The result may be owing to the non-conductive property of enzyme, which hinders the access of the electrons to the electrode (Ji et al., 2010; Yang et al., 2006). With the assembling of CS on the surface of the electrode (curve e), the peak currents have a slight increase compared with the CS-free electrode owing to the weak conductivity of CS. Those results above implied the assembly of ERGO-AuNPs-β-CD, PB-CS, AChE, and CS film on the surface of the electrode.

3.3. Optimization of experimental parameters

Applied potential is an important effect factor on the selectivity and sensitivity of the biosensor. The response current of the biosensor was investigated in the applied potential range from −0.05 to 0.7 V in 0.1 M PBS containing 0.75 mM ATCl, as shown in Fig. 2(A). The results showed that the response current increased with the applied potential increase from 0.05 to 0.2 V and reached a maximum value at 0.2 V, which is similar to the case of the PB-CS modified electrode for the detection of carbaryl at 0.3 V (Song et al., 2011). After that, response current decreased as the further increasing of the applied potential. However, when the applied potential increased from 0.4 to 0.7 V, the response current increased again and reached another maximum at 0.65 V. This result is similar to the case of the biosensors based on CS-PB-multiwall carbon nanotubes (MWNTs)-hollow gold nanospheres (HGNs) (Zhai et al., 2013) and PB (Sun and Wang, 2010) for the detection of OPs at 0.7 V and 0.6 V respectively. The response currents obtained at 0.2 V and 0.65 V are almost same. In order to optimize the optimum applied potential in practical application, the current response of the biosensor was further investigated upon the addition of ATCl and other possible electroactive compounds at 0.2 V and 0.65 V, respectively. As shown in Fig. 2 (B), it can be found the ratios of the signals of the electroactive compounds to the response current of ATCl at 0.2 V were smaller than those at 0.65 V except citric acid, especially for oxalic acid and nitrate. On the basis of these results, an applied potential of 0.2 V was selected for further amperometric experiments and real sample detecting.

Effect of solution pH value and the concentration of AChE on the biosensor was investigated. As shown in Supplementary Information (Fig. S2), the PBS of pH 6.5 and the AChE concentration of 0.5 mg mL^{-1} were selected for the following experiments.

Optimization of ERGO-AuNPs-β-CD film electrodeposition conditions is shown in Supplementary Information (Fig. S3). Electrodeposition potential of −1.4 V, electrodeposition time of 720 s and the concentrations of $HAuCl_4$, β-CD and GO of 1.25 mM, 0.15 mg mL^{-1} and 2.0 mg mL^{-1} were selected, respectively.

3.4. Enhancement effect of PB-CS and ERGO-AuNPs-β-CD on the electrocatalytic oxidation of ATCl

The effect of PB-CS film on the electrocatalytic oxidation of ATCl was investigated by CV. Fig. 3 shows the CVs at differently modified electrodes in the absence and presence of ATCl. At the modified electrode without PB-CS (CS/AChE/ERGO-AuNPs-β-CD/GCE), a small oxidation peak current increase occurred at 0.68 V (Liu and Lin, 2006; Ivanov et al., 2003) after the addition of ATCl (Fig. 3(A)), which is attributed to an oxidation behavior of TCh. In the case of a PB-CS modified electrode (CS/AChE/PB-CS/ERGO-AuNPs-β-CD/GCE), an obviously increasing oxidation peak current was observed at 0.2 V (Arduini et al., 2006; Ricci et al., 2004) after the addition of ATCl (Fig. 3(B)). This might mainly result from the PB nanoparticles toward the electrocatalytic oxidation of TCh. The results above demonstrated that, in the case of PB-CS modified electrode, not only the oxidation currents of TCh increased but also its oxidation potential was shifted to less positive potential (from 0.68 to 0.2 V), indicating that PB could effectively catalyze the oxidation of TCh at low potential. The oxidation of TCh catalyzed

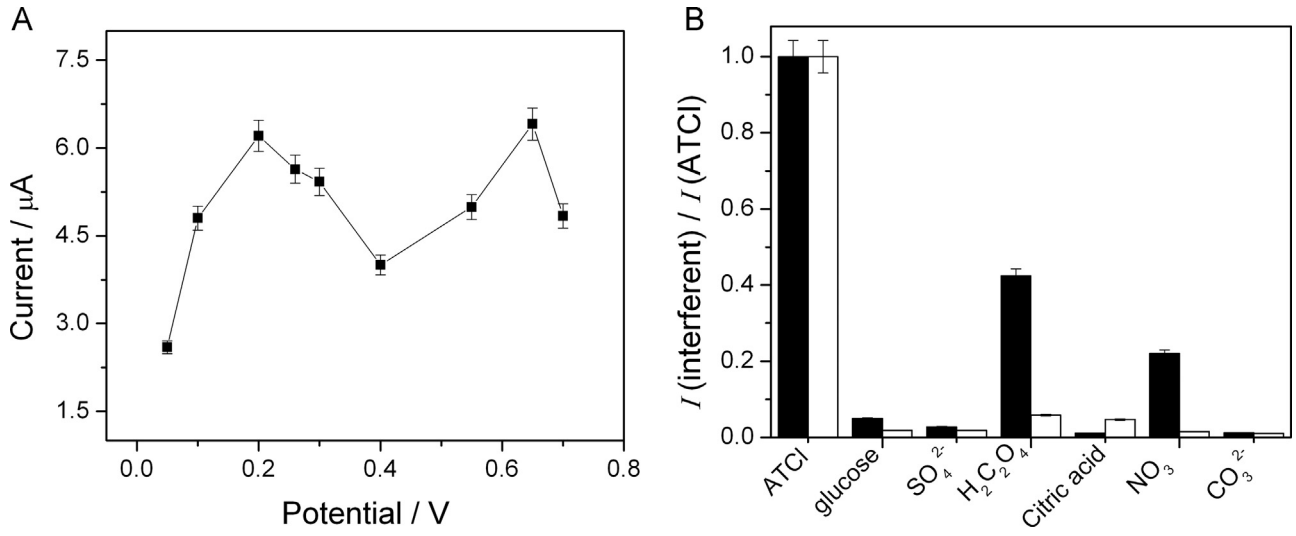

Fig. 2. (A) Effect of applied potential on the response currents of the enzyme biosensor in 0.1 M PBS containing 0.75 mM ATCl. (B) The ratio of the signal for interference to that for ATCl. The response currents was obtained at the biosensor on successive injection of 0.5 mM ATCl, 0.5 mM glucose, 0.5 mM SO_4^{2-}, 0.5 mM $H_2C_2O_4$, 0.5 mM Citric acid, 0.5 mM NO^{3-}, 0.5 mM CO_3^{2-} in 0.1 M PBS at 0.65 V (black) and 0.2 V (white).

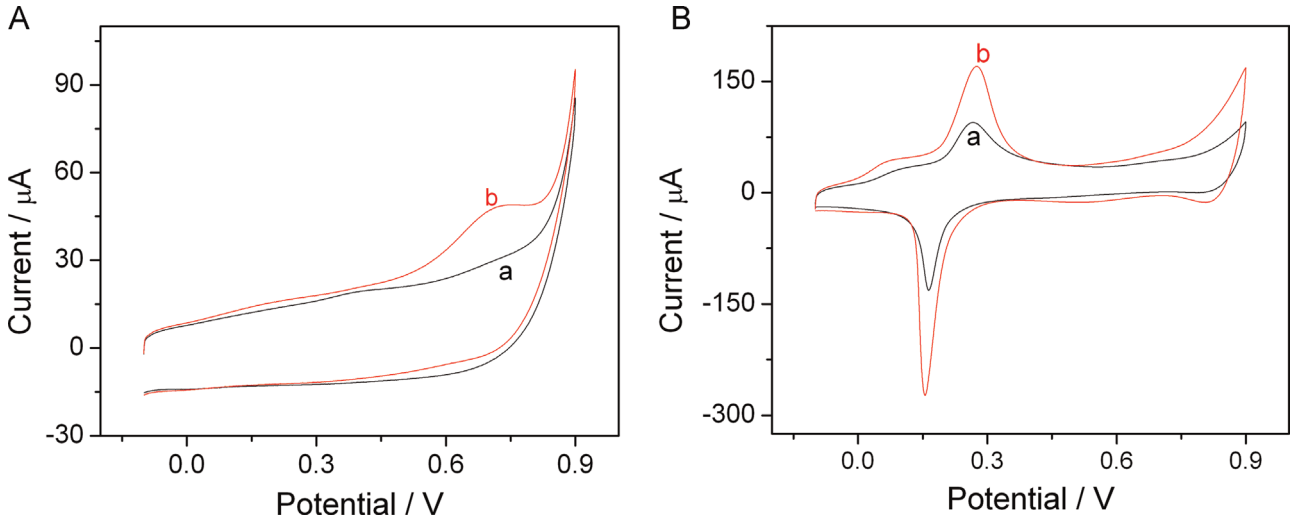

Fig. 3. CVs of CS/AChE/ERGO-AuNPs-β-CD/GCE (A) and CS/AChE/PB-CS/ERGO-AuNPs-β-CD/GCE (B) in 0.1 M PBS (pH 6.5) containing 0.0 mM (a) and 10 mM ATC (b). Scan rate, 20 mV s^{-1}.

by PB nanoparticles could be expressed as follows (Arduini et al., 2006; Ricci et al., 2004).

$$(CH_3)_3N^+CH_2CH_2SC(O)CH_3 + H_2O + AchE \rightarrow (CH_3)_3N^+CH_2CH_2SH + CH_3COOH \quad (2)$$

$$2(CH_3)_3N^+CH_2CH_2SH \rightarrow (CH_3)_3N^+CH_2CH_2SSCH_2CH_2N^+(CH_3)_3 + 2PB_{Red} \quad (3)$$

$$PB_{Red} - 2e^- \rightarrow PB_{OX} \quad (4)$$

In order to investigate the enhancement effect of ERGO-AuNPs-β-CD nanocomposite on the electrocatalytic oxidation of ATCl, two different modified electrodes, with or without ERGO-AuNPs-β-CD, were prepared. The amperometric responses of both two electrodes on successive additions of ATCl in 0.1 M PBS (pH 6.5) at 0.2 V are shown in Fig. 4(A). The oxidation current increased slowly after each addition of 0.2 mM ATCl to the stirred PBS for the electrode without ERGO-AuNPs-β-CD (CS/AChE/PB-CS/GCE, curve a). This is attributed to the oxidation behavior of TCh. However, in the case of ERGO-AuNPs-β-CD modified electrode (CS/AChE/PB-CS/ERGO-AuNPs-β-CD/GCE, curve b), the eletrocatalytic response was very fast. A 95% of steady-state current was achieved within less than 10 s, and the increase of the oxidation current is almost 2.5 times greater than that for CS/AChE/PB-CS/GCE.

The results above demonstrated that the introduction of ERGO-AuNPs-β-CD nanocomposite film dramatically enhanced the electrochemical response of the resulting electrode to ATCl, and the enhancement effect of ERGO-AuNPs-β-CD nanocomposite on the response current was also related to the enzyme. This may be explained as follows. Firstly, the enhanced electrochemical response can be ascribed to the superb physicochemical property of ERGO (Kim et al., 2009). The good conductivity and small band of ERGO could effectively promote the electrocatalysis toward TCh. AuNPs, having unique chemical and physical properties (Batra and Pundir, 2013; Hou et al., 2012), could facilitate electron transfer and produce signal amplification in electrochemical detection. Secondly, the high surface area of ERGO and AuNPs are contribute to the increase of the surface loading of AChE. ERGO and AuNPs could also provide a favorable microenvironment for the enzyme to maintain the biological activity of the AChE. Thirdly, the synergistic effect of ERGO, AuNPs and PB nanocomposites could promote the electron transfer between PB and GCE, and enhance the electrochemical oxidation of TCh at the electrode surface.

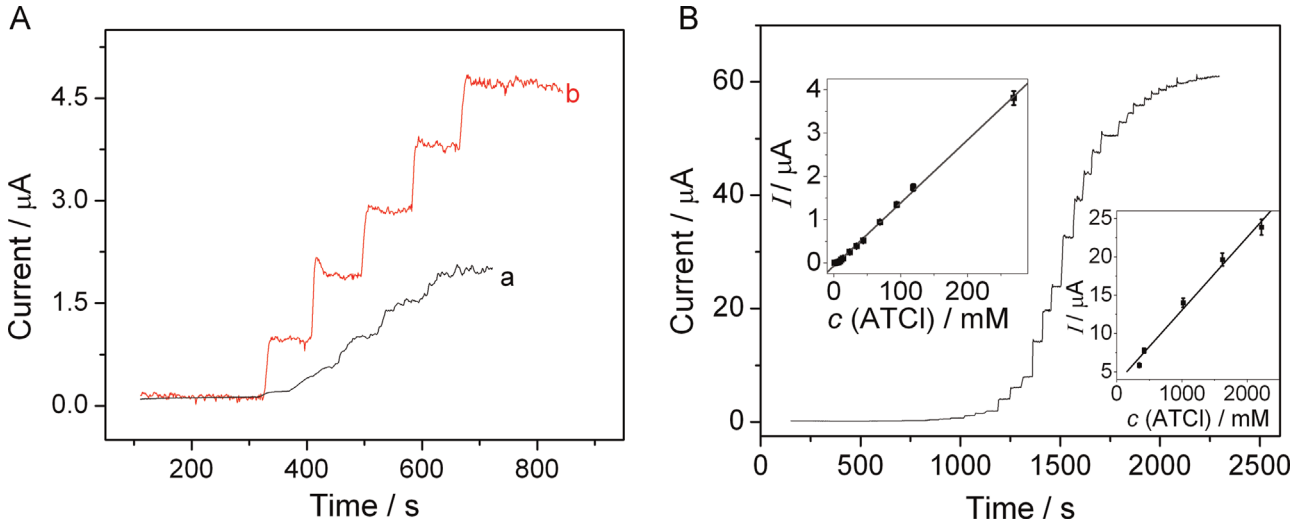

Fig. 4. Amperometric responses of (A) CS/AChE/PB-CS/GCE (a), CS/AChE/PB-CS/ERGO-AuNPs-β-CD/GCE (b) in 0.1 M PBS (pH 6.5) with consecutive addition of 0.2 mM ATCl and (B) CS/AChE/PB-CS/ERGO-AuNPs-β-CD/GCE in 0.1 M PBS (pH 6.5) on successive injection of 1.5, 2.0, 2.5, 10, 25, 50, 80, 5.0×10^2, 6.0×10^2 and 1.5×10^3 μM ATCl. (Inset, linear calibration between the current response and ATCl concentration). Applied potential, 0.2 V vs. Ag/AgCl (3 M KCl).

Besides, β-CD could interact with ATCl by reversible bonding, which is contribute to increase the enrichment of ATCl, and improve the selectivity and sensitivity of the biosensor (Lee et al., 2008).

3.5. Amperometric response of the biosensor toward ATCl

The amperometric response of the biosensor to ATCl in 0.1 M PBS at an applied potential of 0.2 V is shown in Fig. 4(B). It can be found that upon the injection of an aliquot of ATCl, the oxidation current increased and then reached a stable value rapidly. A 95% of steady-state current was achieved within less than 10 s, which clearly illustrated that the eletrocatalytic response was very fast. The response current of the biosensor was proportional to the concentration of ATCl in two ranges, from 1.50 to 2.69×10^{2} μM and from 3.44×10^{2} to 2.22×10^{3} μM (Fig. 4(B), inset). The linear equations were I (μA)=14.5c(mM)+6.48×10^{-2} (R=0.999) and I (μA)=9.51c(mM)+3.54 (R=0.994). The corresponding sensitivities, determined as the slope of the linear calibration curve (dI/dc), were 14.5 and 9.51 μA mM^{-1}. The sensitivity of this biosensor has been significantly improved, compared with previously reported (Zhai et al., 2013). With a further increase in ATCl concentration, a response plateau appeared, showing the characteristics of Michaelis–Menten kinetics. The apparent Michaelis–Menten constant (K_m^{app}) was calculated to be 1.06×10^{-1} mM according to the Lineweaver–Burk equation (Shu and Wilson, 1976; Kamin and Wilson, 1980). The K_m^{app} for the biosensor is much smaller than those obtained from other recent reports (Zhai et al., 2013; Wang et al., 2011). A small K_m^{app} implies that the AChE immobilized on the electrode retains its catalytic activity and displays a higher affinity for ATCl.

3.6. Application of the biosensor for pesticides determination

In the present work, malathion and carbaryl were selected as the typical ones of organophosphorus and carbamate pesticides respectively to test the performance of the resulting biosensor.

The effect of different concentrations of malathion on the activity of immobilized AChE was investigated by CV under optimal conditions. Fig. 5(A) shows the response current of the CS/AChE/PB-CS/ERGO-AuNPs-β-CD/GCE in 0.1 M PBS (pH 6.5) containing 10 mM ATCl after inhibited by different concentrations of malathion for 10 min (optimization of inhibition time is shown in Fig. S4). As the increase of the concentration of malathion, the oxidation peak current decreased successively at 0.2 V. This is ascribed to the fact of the decrease of AChE activity, which resulted in the decrease of TCh. The inhibition of malathion on the activity of AChE rapidly increased at first with the increase of the concentration of malathion, then trended to a stable value as its concentration was more than 390 pg mL^{-1}, indicating that the interaction between malathion and active target groups in AChE reached saturation. The concentration of OPs can be precisely detected by measuring decline of the oxidation peak current of TCh.

The proposed electrode was employed for the pesticides determination by DPV at 0.2 V. Fig. 5(B) shows the DPV response of the biosensor before or after exposure to different concentrations of malathion. The oxidation peak current decreased at 0.2 V with the increase of the concentration of malathion due to the inhibition of AChE by malathion. As shown in Fig. 5(B, Inset), under optimal conditions, the inhibition was proportional to the concentrations of malathion and carbaryl in the ranges of 7.98 – 2.00×10^{3} pg mL^{-1} and 4.3 – 1.00×10^{3} pg mL^{-1}, with the detection limits of 4.14 pg mL^{-1} and 1.15 pg mL^{-1} respectively. The analytical performance of the resulting biosensor was compared with other reported AChE biosensors, and the results are summarized in Table 1. The results showed that this biosensor exhibited a higher sensitivity, a lower detection limit and a wider range.

3.7. Regeneration of AChE and stability and repeatability of the biosensor

AChE reactivation was investigated with pralidoxime iodide as activity recovery agent. After the biosensor was inhibited by malathion, it was immersed in 5.0 mM pralidoxime iodide for 15 min. As shown in Fig. S5, the inhibited AChE could be regenerated more than 94.2% of its original activity. The proposed biosensor exhibited an acceptable reproducibility in repeated use. The repeatability of the biosensor was also investigated with the same electrode by 6 times successive amperometric measurements, and the relative standard deviation (RSD) was found to be 4.27%, which proved a good repeatability. When the enzyme electrode was not in use, it was stored in 0.1 M PBS of pH 6.5 at 4 °C. The response current of the enzyme electrode only decreased by 8% of its initial response after 28 days, showing a good storage stability.

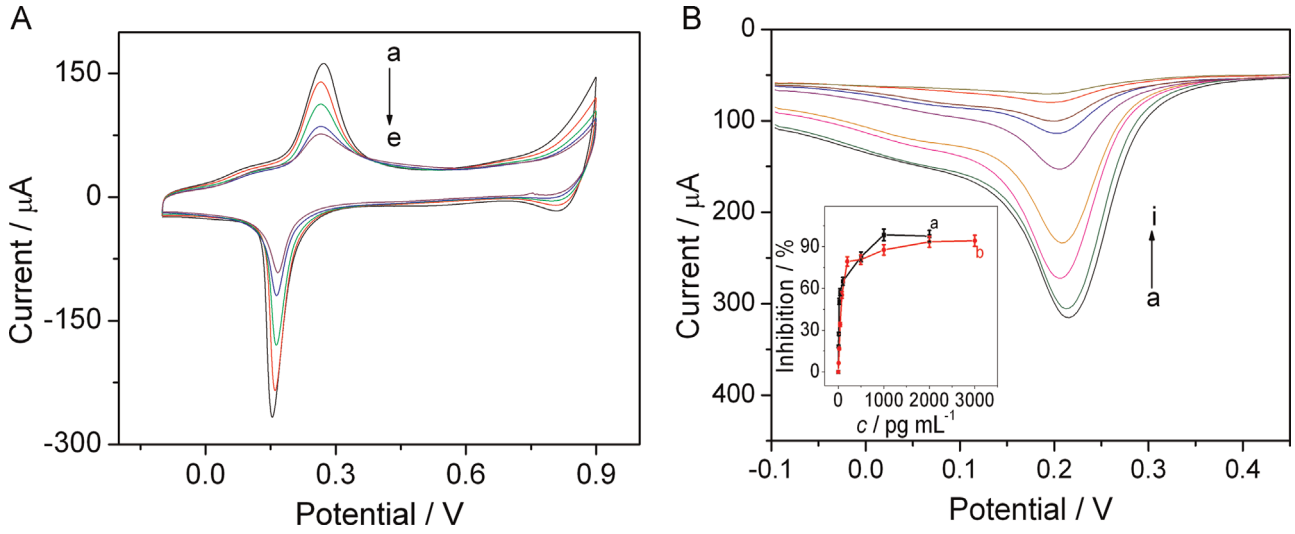

Fig. 5. CV (A) and DPV (B) of the biosensor in 0.1 M PBS (pH 6.5) containing 10.0 mM ATCl after inhibition with malathion for 10 min. Malathion concentration (A, a–e): 0, 12, 195, 390, 585 pg mL^{-1}, (B, a–i): 0; 7.98; 20; 40; 80; 198; 495; 1000; 2000; 3000 pg mL^{-1}. Inset (B), relationship between inhibition rate and malathion (a) and carbaryl (b) concentration.

Table 1
Analytical characteristics of graphene-based biosensors for pesticides.

Electrode	Linear range	Sensitivity ($\mu A\ mM^{-1}$)	K_m (mM)	Detection limit	Ref.
CS/AChE/PB-CS/ERGO-AuNPs-β-CD/GCE	7.98–2000[a], 4.3–1000[b] pg mL^{-1}	14.5, 9.51	0.106	4.14[a] , 1.15[b] pg mL^{-1}	This work
AChE/PB-CS/GCE	0.01–5.0 μM [b]	–	–	3[b] nM	Song et al. (2011)
Nafion/AChE/CS-PB-MWNTs-HGNs/Au	0.05–75[a], 0.05–75[c], 0.1–50[d], 5–80[e] nM	5.1	0.21	0.05[a], 0.05[c], 0.1[d], 2.5[e] nM	Zhai et al. (2013)
AChE/CPBA/GR-AuNPs/GCE	0.5–100[a], 0.5–100[c], 0.1–100[e], 2–10[f] ppb	16, 5.6	0.16	0.5[a], 0.1[c], 0.05[e], 0.5[f] ppb	Liu et al. (2011)
AChE-MWCNTs-Au-CS/GCE	1.0–1000[a] ng mL^{-1}	–	0.27	0.6[a] ng mL^{-1}	Du et al. (2010)

CPBA: 3-carboxyphenylboronic.

[a] Malathion.
[b] Carbaryl.
[c] Chlorpyrifos.
[d] Monocrotophos.
[e] Carbofuran.
[f] Isoprocarb.

3.8. Real sample analysis

To investigate the possible application of the developed biosensor in real samples analysis, the CS/AChE/PB-CS/ERGO-AuNPs-β-CD/GCE was employed to the recovery tests by adding different amounts of pesticides into vegetables. The results are listed in Table S1. The recoveries for the determination of malathion and carbaryl were from 92.8% to 106.7% and from 90.3% to 101.5%, respectively. The results indicated that the biosensor exhibited a good accuracy for the pesticides sensing in real samples and a great potential for practical application.

4. Conclusion

An ultra-sensitive amperometric OPs biosensor was successfully fabricated by immobilizing AChE on ERGO-AuNPs-β-CD/PB-CS nanocomposites film-modified GCE. The combination of ERGO with AuNPs co-electrodeposited on GCE efficiently promoted the electron transfer between the analyte and the electrode surface and improved the performance of the biosensor due to the virtue of the electrocatalytic synergy effect between them. On the other hand, ERGO and AuNPs were also contribute to increase the surface loading of AChE, and provided a suitable microenvironment for the immobilization of AChE. Besides, PB not only enhanced the oxidation currents of TCh, but also shifted its oxidation potential toward less positive potentials in contrast to PB-free modified GCE, and accordingly the sensitivity of biosensor was largely improved. The resulting ERGO-based enzyme biosensor exhibited excellent sensitivity, good stability, fast electrochemical response and good reproducibility.

Acknowledgements

This work was financially supported by the Natural Science Foundation of Hebei Province of China (No. B2010000844) and Research Foundation of Education Department of Hebei Province of China (No. ZH2012078).

Appendix A. Supplementary material

Supplementary data associated with this article can be found in the online version at http://dx.doi.org/10.1016/j.bios.2014.10.007.

References

Abad, J.M., Pariente, F., Hernández, L., Abruna, H.D., Lorenzo, E., 1998. Anal. Chem. 70, 2848–2855.
Allen, M.J., Tung, V.C., Kaner, R.B., 2010. Chem. Rev. 110, 132–145.
Arduini, F., Ricci, F., Tuta, C.S., Moscone, D., Amine, A., Palleschi, G., 2006. Anal. Chim. Acta 580, 155–162.
Bai, X., Chen, G., Shiu, K., 2013. Electrochim. Acta 89, 454–460.
Batra, B., Pundir, C.S., 2013. Biosens. Bioelectron. 47, 496–501.
Brownson, D.A.C., Banks, C.E., 2010. Analyst 135, 2768–2778.
Chiu, J., Yu, C., Yen, M., Chen, L., 2009. Biosens. Bioelectron. 24, 2015–2020.
Du, D., Wang, M., Cai, J., Tao, Y., Tu, H., Zhang, A., 2008. Analyst 133, 1790–1795.
Du, D., Ye, X., Cai, J., Liu, J., Zhang, A., 2010. Biosens. Bioelectron. 25, 2503–2508.
Gan, T., Hu, S., 2011. Microchim. Acta 175, 1–19.
Guan, H.X., Brewer, W.E., Garris, S.T., Morgan, S.L., 2010. J. Chromatogr. A 1217, 1867–1874.
Guo, S., Dong, S., Wang, E., 2010. ACS Nano 4, 547–555.
Hou, S., Ou, Z., Chen, Q., Wu, B., 2012. Biosens. Bioelectron. 33, 44–49.
Hummers, W.S., Offeman, R.E., 1958. J. Am. Chem. Soc. 80, 1339.
Hu, Y., Jin, J., Wu, P., Zhang, H., Cai, C., 2010. Electrochim. Acta 56, 491–500.
Ivanov, A., Evtugyn, G., Budnikov, H., Ricci, F., Moscone, D., Palleschi, G., 2003. Anal. Bioanal. Chem. 377, 624–631.
Ji, X., Ren, J., Ni, R., Liu, X., 2010. Analyst 135, 2092–2098.
Kamin, R.A., Wilson, G.S., 1980. Anal. Chem. 52, 1198–1205.
Kim, K.S., Zhao, Y., Jang, H., Lee, S.Y., Kim, J.M., Kim, K.S., Ahn, J.H., Kim, P., Choi, J.Y., Hong, B.H., 2009. Nature 457, 706–710.
Lee, C., Wei, X., Kysar, J.W., Hone, J., 2008. Science 321, 385–388.
Liu, G., Lin, Y., 2006. Anal. Chem. 78, 835–843.
Liu, K., Zhang, J., Yang, G., Wang, C., Zhu, J., 2010a. Electrochem. Commun. 12, 402–405.
Liu, S., Wang, J., Zeng, J., Ou, J., Li, Z., Liu, X., Yang, S., 2010b. J. Power Sources 195, 4628–4633.
Liu, T., Su, H., Qu, X., Ju, P., Cui, L., Ai, S., 2011. Sens. Actuators B 160 (1255–126).
Li, Y., Bai, Y., Han, G., Li, M., 2013. Sens. Actuators B 185, 706–712.
Morozov, S.V., Novoselov, K.S., Katsnelson, M.I., Schedin, F., Elias, D.C., Jaszczak, J.A., Geim, A.K., 2008. Phys. Rev. Lett. 100, 016602/1–016602/4.
Novoselov, K.S., Geim, A.K., Morozov, S.V., Jiang, D., Zhang, Y., Dubonos, S.V., Grigorieva, I.V., Firsov, A.A., 2004. Science 306, 666–669.
Ou, C., Yuan, R., Chai, Y., Tang, M., Chai, R., He, X., 2007. Anal. Chim. Acta 603, 205–213.
Rekha, K., Thakur, M.S., Karanth, N.G., 2000. Crit. Rev. Biotechnol. 20, 213–235.
Ricci, F., Arduini, F., Amine, A., Moscone, D., Palleschi, G., 2004. J. Electroanal. Chem. 563, 229–237.
Shu, F.R., Wilson, G.S., 1976. Anal. Chem. 48, 1679–1686.
Song, Y., Zhang, M., Wang, L., Wan, L., Xiao, X., Ye, S., Wang, J., 2011. Electrochim. Acta 56, 7267–7271.
Song, H., Ni, Y., Kokot, S., 2013. Anal. Chim. Acta. 788, 24–31.
Sun, C., Lee, H.H., Yang, J., Wu, C., 2011. Biosens. Bioelectron. 26, 3450–3455.
Sun, W., Cao, L., Deng, Y., Gong, S., Shi, F., Li, G., Sun, Z., 2013. Anal. Chim. Acta 781, 41–47.
Sun, X., Wang, X., 2010. Biosens. Bioelectron. 25, 2611–2614.
Tan, Y., Deng, W., Chen, C., Xie, Q., Lei, L., Li, Y., Fang, Z., Ma, M., Chen, J., Yao, S., 2010. Biosens. Bioelectron. 25, 2644–2650.
Wang, B., Ji, X., Zhao, H., Wang, N., Li, X., Ni, R., Liu, Y., 2014. Biosens. Bioelectron. 55, 113–119.
Wang, K., Liu, Q., Dai, L., Yan, J., Ju, C., Qiu, B., Wu, X., 2011. Anal. Chim. Acta. 695, 84–88.
Wu, Y., Niu, H., Wang, K., Liu, Q., Li, H., Dong, X., Zhao, K., Zhu, Y., 2013. Sensor Lett. 11, 436–441.
Yang, J., Myoung, N., Hong, H., 2012. Electrochim. Acta 81, 37–43.
Yang, W., Wang, J., Zhao, S., Sun, Y., Sun, C., 2006. Electrochem. Commun. 8, 665–672.
Ye, J., Wu, J., Liu, W., 2009. Trends Anal. Chem. 28, 1148–1163.
Zeng, J., Wei, W., Liu, X., Wang, Y., Luo, G., 2008. Microchim. Acta 160, 261–267.

Zhai, C., Sun, X., Zhao, W., Gong, Z., Wang, X., 2013. Biosens. Bioelectron. 42, 124–130.
Zhao, S., Zhang, K., Bai, Y., Yang, W., Sun, C., 2006. Bioelectrochemistry 69, 158–163.
Zhou, K., Zhu, Y., Yang, X., Luo, J., Li, C., Luan, S., 2010. Electrochim. Acta 55, 3055–3060.
Zhou, Q., Yang, L., Wang, G., Yang, Y., 2013. Biosens. Bioelectron. 49, 25–31.